Geotech Geol Eng (2022) 40:5507–5525
https://doi.org/10.1007/s10706-022-02229-z

ORIGINAL PAPER

A Semi-Empirical Approach for Rockfall Prediction Along the Lengpui-Aizawl Highway Mizoram, India

Sahil Sardana · Rabindra Kumar Sinha · A. K. Verma · Mamta Jaswal · T. N. Singh

Received: 7 December 2021 / Accepted: 17 June 2022 / Published online: 9 July 2022

Abstract The Lengpui-Aizawl highway in the Northeastern part of India has witnessed several rockfall events in the past decades. This is the only highway that connects the Airport to the city. Considering the importance of the highway, semi-empirical equations were developed to predict the rockfall output parameters such as bounce height, velocity and kinetic energy. The five major input parameters, such as slope height, slope-angle, slope-roughness, block-weight and coefficient of restitution that can affect the rockfall, have been considered for the parametric study. The paper includes detailed site investigation, laboratory investigation and rockfall modelling to estimate the generalised equations based on multivariate linear regression analysis. The site survey includes topographical and geological details of 13 rock slopes along the Lengpui-Aizawl highway. The coefficient of restitution was estimated in the laboratory using a fabricated rockfall setup. Further, 243 modellings were performed to analyse the data and develop the generalised rockfall equations. These generalised equations will help the field engineers to predict the outcome of the rockfall activity and help design suitable mitigative measures.

Keywords Restitution coefficient · Design of experiment · Bounce height · Rockfall barrier · Mitigative measures · Aizawl

S. Sardana (✉) · R. K. Sinha · M. Jaswal
Department of Mining Engineering, Indian Institute of Technology (Indian School of Mines), Dhanbad, Jharkhand 826004, India
e-mail: sahilsardana.ymca@gmail.com

S. Sardana
Maccaferri Environmental Solutions Private Limited, Gurugram, Haryana 122001, India

A. K. Verma
Department of Mining Engineering, Indian Institute of Technology (Banaras Hindu University), Varanasi, Uttar Pradesh 221005, India

T. N. Singh
Department of Earth Sciences, Indian Institute of Technology Bombay, Maharashtra 400076, India

1 Introduction

Rockfall is a significant hazardous event in the hilly regions as it has the potential to damage infrastructures and causes severe injuries or fatalities (Badger and Lowell 1992). The geotechnical setup and geodynamic behaviour of the slopes are responsible for the frequency of landslides in the Himalayan region (Kumar et al. 2018). The failure in slopes is governed by numerous factors such as geomorphological features (Hoek and Bray 1981), freeze–thaw cycle (McCarroll et al. 1998), seismic activities (Valagussa et al. 2014), rainfall/groundwater (Jaswal et al. 2020; Wei et al. 2014) and vegetation. The study conducted by Wyllie and Norrish (1996) reveals that rainstorms cause 30% of the rockfall activities, 21% due to the

freeze–thaw process, and the remaining due to fractured rock, wind, etc.

Asteriou et al. (2012) describe that rockfall activity depends on numerous factors, such as slope characteristics i.e. slope height, slope angle, slope roughness etc., block characteristics i.e. block mass, block shape, block size, block strength etc. Recently, Dattola et al. (2021) investigated the effect of shape and rotation motion on the rockfall impacts based on visco-plastic theory. The higher slope height tends to increase the kinetic energy associated with the falling rock blocks. The slope angle affects the rockfall trajectory and the shear stress acting on the potential failure plane (Roth 1983). Slope excavation is one of the main factors causing an alteration in slope geometry (McColl 2015). The various types of rockfall motions, such as fall, roll and bounce, occur after separating a rock block from the detachment point (Ritchie 1963). The trajectories of falling rock blocks can be influenced by the coefficient of restitution (CoR), roughness of the slope surface, coefficient of rolling friction and the coefficient of sliding friction. Irfan and Chen (2017) developed mathematical equations to predict the rockfall trajectories.

CoR is defined as the ratio of the velocities before and after the impact of rock block on the slope's surface. In the rockfall modelling, normal and tangential CoR (R_n and R_t) are being used separately to calculate the rebound velocity components in the normal and tangential direction (Wu 1985). Richards (1988) observed that the values of CoR (especially R_n) have a substantial effect on the rockfall trajectories. The value of R_n and R_t are used to quantify the energy dissipation during an impact in the prediction of rockfall (Buzzi et al. 2012). Asteriou (2019) demonstrates the influence of rockfall impact and rotational motion on the CoR. Slope roughness is characterized by the waviness and unevenness of the slope (ISRM 1981). The large-scale waviness contributes to resistive shear stress. These irregularities in the slope surface are responsible for variation in rockfall trajectories, as they alter the impact angle. Slope roughness plays a crucial role in the rockfall assessment. Verma et al. (2018) performed the sensitivity analysis that shows it affects the rockfall assessment outcome. Rolling friction coefficient (μ_r) represents the slope's resistance to the angular velocity of the rock block, whereas sliding friction coefficient (μ_s) represents the resistance offered by the slope surface to the sliding of the rock block. The rolling motion is restricted to a limiting angle of inclination. Peng (2000) investigated the characteristics of μ_r by varying the value of θ_r ranging from 1° to 5°, and observed that under the rolling conditions, coefficient of rolling friction does not play a significant role. It is actually the coefficient of sliding friction that offers a significant resistance to the movement of the rock block as compared to the coefficient of rolling friction.

A major part of the study was concentrated along the NH-44A highway since it is a lifeline of the Aizawl city, as this is the only link between the Aizawl city to the Lengpui Airport. The stability of rock slopes in the vicinity of Aizawl city varies from partially stable to unstable (Sardana et al. 2019a; 2019b). The preliminary study, based on Rockfall Hazard Rating System (RHRS) carried out by Verma et al. (2021), shows that the road cuts along the Lengpui-Aizawl highway are prone to rockfall and comes under moderate to higher urgency. Hoek (1999) allocated the rockfall hazard rating into three categories of urgency: high, medium and low, indicating the extent of the hazard. The slopes with RHRS scores higher than 500 require immediate attention. Based on RHRS scores, the slopes along the Lengpui-Aizawl highway are highly vulnerable and a continuous threat to the rockfall. Therefore, these slopes required a detailed rockfall assessment. Moreover, this highway has witnessed several rockfall events in the past few years (Sardana et al. 2020; Verma et al. 2019; Lallianthanga et al. 2013). The present work aims to develop a set of equations using parametric analysis to determine the rockfall output parameters: bounce height, velocity, and kinetic energy. The equations were developed using multivariate linear regression to guide predicting risk assessment concerning the bounce height, velocity, and energy accompanying the falling rock blocks. These equations serve the purpose of input parameters required by engineers associated with designing suitable mitigative measures against the adverse effect of rockfall.

2 Field Investigations

2.1 Location

The slopes under investigation are located along the Lengpui-Aizawl highway (NH-44A). The field study covers a total of 13 rock slopes from Lengpui Airport toward Aizawl city. The stretch located between the latitudes 23° 50′ 19.85″*N*–23° 46′ 52.95″*N* and longitudes 92° 37′ 27.01″*E*–92° 40′ 35.23″*E*. The study area comes under toposheet no. 83D/15, 84A/10, and 83H/4 of the Survey of India. The highway is constantly under the threat of rockfall activity at an elevation ranging from 273 to 413 m. The coordinates and elevation of the rock slopes are reported in Table 1.

2.2 Geology

The geological investigation reveals that the area is predominantly overlain by Neogene sedimentary rocks of Tipam and Surma group formation. In Mizoram, the sedimentary column is a repetitive succession of arenaceous and argillaceous rocks comprising sandstone, shale, mudstone, silty-sandstone, silty-shale and their mixtures. Surma group covers a large portion and is subdivided into Bhuban and Bokabil formations. Bhuban formation is further divided into Upper, Middle and Lower Bhuban (Ganju 1975). The entire Aizawl city includes top and middle Bhuban dispositions of the Surma group of rocks (Kesari 2011). This group of rocks

Table 1 Details of road cuts along the Lengpui-Aizawl highway

Slopes	Latitude- Longitude	Elevation (m)	Slope height (m)	Stretch length (m)	Slope angle (deg)	Average in-situ UCS (MPa)	Lithology
L-1	23° 49′ 09″ *N* 92° 37′ 32″ *E*	273	30	90	85–90	41	Shale and Sandstone
L-2	23° 48′ 35″ *N* 92° 37′ 18″ *E*	228	10	15	85–90	35	Shale
L-3	23° 48′ 27.23″ *N* 92° 39′ 40.01″ *E*	209	12	45	75–80	30.5	Shale
L-4	23° 48′ 22.97″ *N* 92° 39′ 40.92″ *E*	220	9	30	85–90	34.5	Shale
L-5	23° 48′ 1.49″ *N* 92° 39′ 53.2″ *E*	264	5	35	80–85	23.5	Sandstone and Shale
L-6	23° 47′ 55.03″ *N* 92° 39′ 58.04″ *E*	284	11	25	85–90	31	Siltstone with shale
L-7	23° 47′ 50.62″ *N* 92° 39′ 53.51″ *E*	306	10	9	70–75	30	Siltstone and sandstone
L-8	23° 47′ 43.41″ *N* 92° 39′ 52.96″ *E*	309	15	40	75–80	38	Siltstone and sandstone
L-9	23° 47′ 04.88″ *N* 92° 40′ 21.42″ *E*	413	10	35	80–85	32.5	Siltstone and Shale
L-10	23° 47′ 02.88″ *N* 92° 40′ 24.45″ *E*	430	9	25	85–90	34	Shale and Sandstone
L-11	23° 47′ 00.79″ *N* 92° 40′ 26.00″ *E*	434	10	30	75–80	33.5	Shale and Sandstone
L-12	23° 46′ 57.88″ *N* 92° 40′ 28.29″ *E*	423	31	110	85–90	36.5	Shale and Sandstone
L-13	23° 46′ 52.95″ *N* 92° 40′ 35.23″ *E*	431	15	45	75–80	32.5	Shale and Siltstone

embraces alternate shale beds, siltstone, sandstone and mudstone of diverse thicknesses. Sandstones are hard, compact and stable, whereas shale beds are brittle compared to sandstone. They include bands of micaceous-felspathic and weathered sandstone (Lallianthanga et al. 2013). An arenaceous and argillaceous batch of rocks lies in relatively upper and lower ground, respectively. Reconnaissance traversing from Aizawl to Champhai resulted in identifying a Barail batch of rocks in and around the Champhai subdivision, Aizawl district, and Bhuban in the west. The geological map of the study area is shown in Fig. 1.

2.3 Site Characterization

Extensive site characterization includes estimating slope height, slope angle, slope geometry, slope orientation, joint orientation and discontinuity conditions and the dimension of potential falling rock blocks. Figure 2 and 3 shows the field photographs of rock slopes along this highway. Figure 4 shows the different sizes of rock blocks observed at the site. The topographical and lithological details have been provided in Table 1. Slope angle, weight of falling blocks and slope height are major parameters that affect the falling blocks' path and energy. Therefore, the histograms have been plotted, showing the values for the three factors mentioned above (Fig. 5). The height of the slope varied from 5 to 31 m; therefore, the slope height has been divided into three categories, ≤ 10 m, 11–20 m and > 20 m (Fig. 5a). Similarly, the data was divided into three categories, for slope-angle, $\leq 75°$, 75–85° and $> 85°$ (Fig. 5b); and for block-weight, ≤ 300 kg, 300–800 kg, and > 800 kg (Fig. 5c). An average height and a range of angles have been considered for 13 rock slopes for the slope height and slope-angle parameter. The block weight was estimated to consider approximately 150 fallen rock blocks observed during the site investigation.

3 Laboratory Investigations

The restitution coefficient (CoR) plays a crucial role in the rockfall assessment. It is associated with the dissipation of energy in the course of the impact. The normal restitution coefficient (R_n) has been

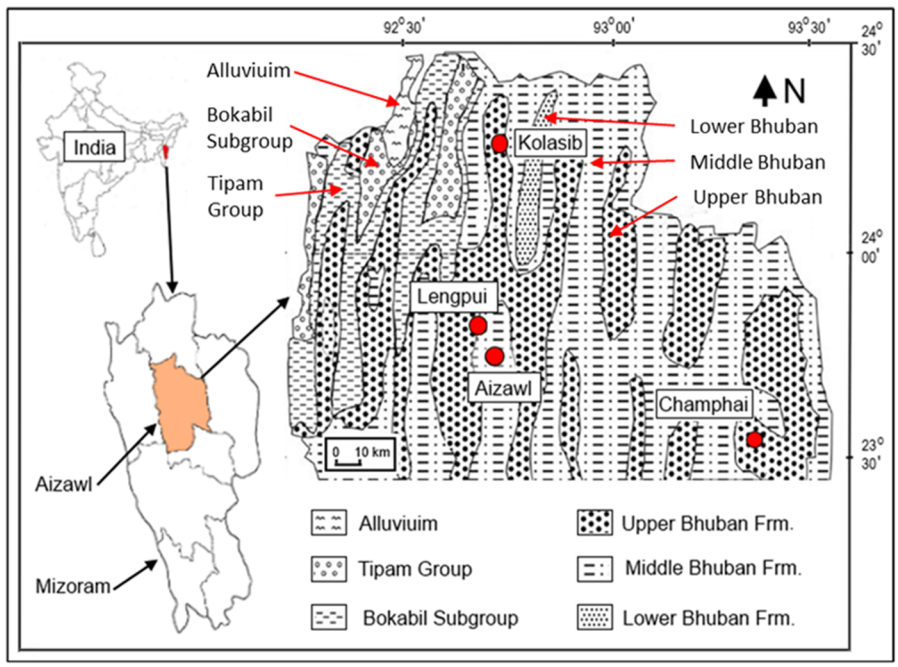

Fig. 1 Geological map of Mizoram showing Aizawl and Lengpui area (after Ram and Venkataraman 1984)

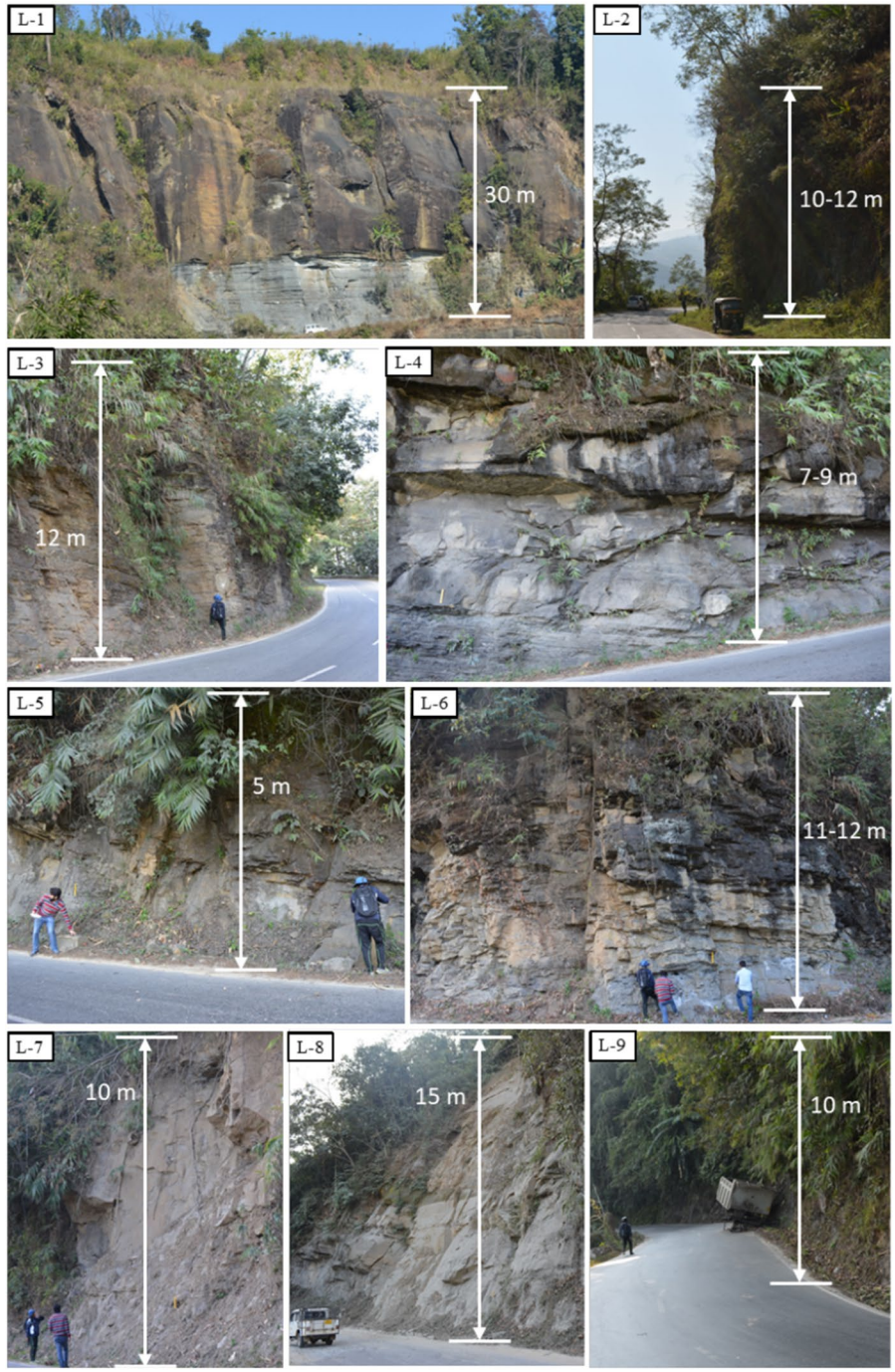

Fig. 2 Field photographs showing road cuts (L-1–L-9) along NH-44A, Aizawl

determined in the laboratory using a setup (Fig. 6). The experimental setup consists of a steel frame with a releaser fixed at the top and a base casing to accommodate the rock slab. The height of the releaser can be varied by adjusting the threaded rod attached to it. The supporting frame is mounted with a scale of 1 m length graduated in millimetres. The resting slab's angle can be varied by adjusting the pinion attached

Fig. 3 Field photographs showing road cuts (L-10–L-13) along NH-44A, Aizawl

to the base frame (Fig. 6). A high-speed camera was used for image exposures in excess of 1/1000 or frame rates of more than 250 frames per second. It was used to record fast-moving objects as photographic images onto a storage medium. After recording, the images stored on the medium can be played back in slow-motion.

The rock slab was placed under the sample holder and a high-speed camera was fixed parallel to the setup. The almost spherically shaped small rock sample was kept in the holder and released such that it experienced a free fall with a drop height of 0.66 m and bounced on the approximately rectangular rock slab. The test was repeated on the same rock slab with

Fig. 4 Field photographs showing falling rock blocks along NH-44A, Aizawl

different small rock pieces. The camera captured the motion; later, the recorded video was transferred to the computer and analysed by the motion tracking software (Tracker software).

The maximum positive value of V_f and maximum negative value of V_i has been taken to estimate R_n as per Eq. 1.

$$R_n = \frac{V_f}{V_i} \tag{1}$$

where V_f and V_i are the velocities of the falling rock block, after and before the bounce on the rock slab. Ten values have been plotted in Fig. 7 determined from the CoR setup, which shows 50% of the values come under less than 0.46 CoR, 20% higher than 0.5 CoR and the remaining values fall between 0.46 and 0.5.

4 Rockfall Modelling

The rockfall modelling has been performed using the RocFall software package from Rocscience. The analysis in this package is based on either lumped mass or rigid body approach. In the lumped mass approach, each rock block is considered as a very small spherical particle. Therefore, the rock block's mass is considered, and the size or shape is not considered in the analysis. In contrast, the rigid body approach considers the shape and size of the rock block depending on its mass. The critical input parameters considered in the rockfall modelling are slope height, slope angle, rock block weight, source of the rockfall (i.e. seeder point), CoR and slope roughness. The major output parameters determined in the rockfall analysis are its trajectories, bounce height, velocity and energy at any point.

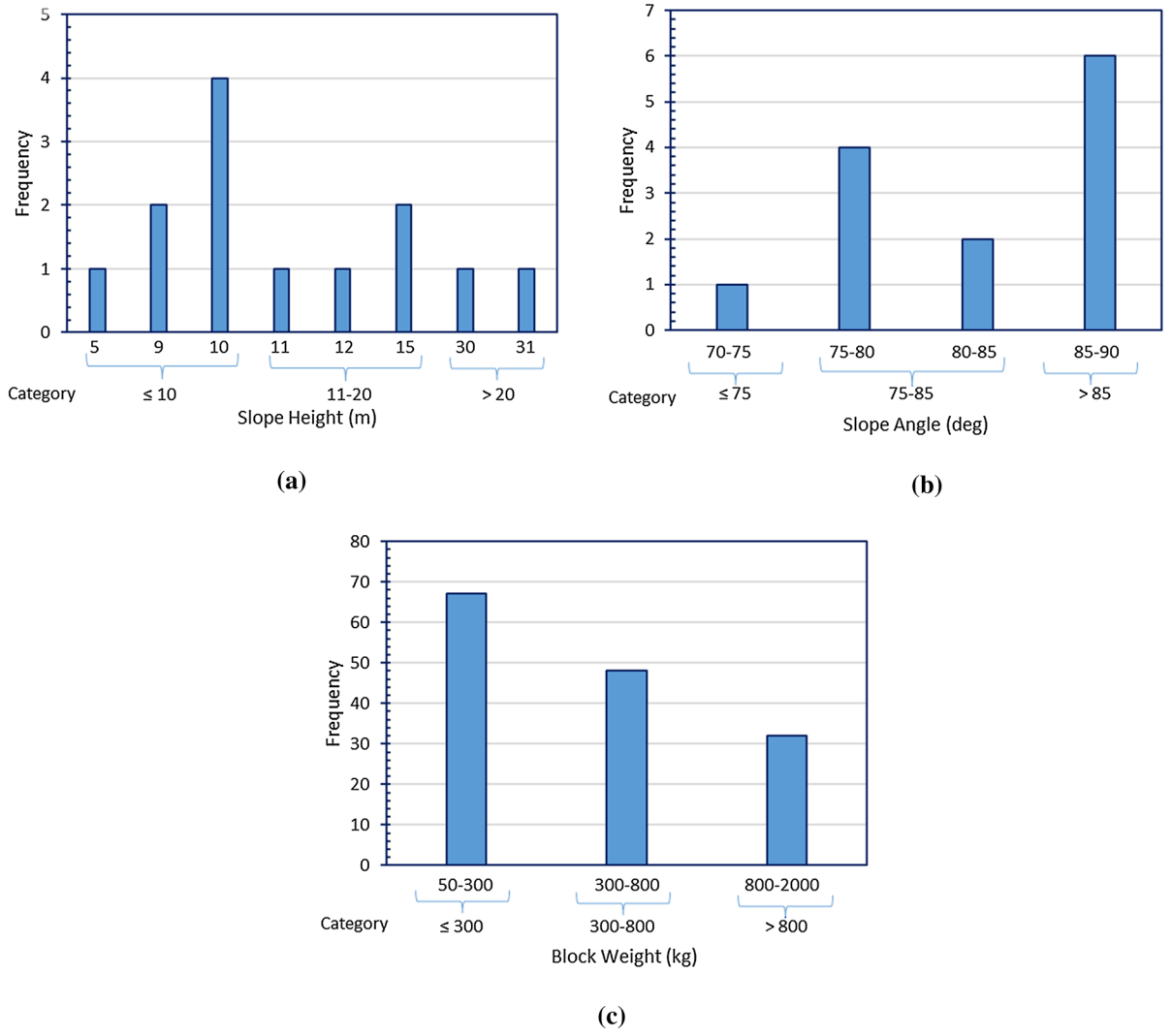

Fig. 5 Histogram plots showing the frequency of **a** slope height, **b** slope angle and **c** weight of the falling rock blocks

In this study, rockfall modelling has been performed using lumped mass formulation. The values of slope height (10–30 m), slope angle (65–85 deg) and the weight of the block (100–1000 kg) have been estimated based on extensive field investigations (Figs. 2, 3, 4). The normal restitution coefficient values have been estimated in the laboratory (Fig. 6) and the range of slope roughness has been considered from the literature (Verma et al. 2018; RocScience 2016; Srikanth 2015). Figure 8 shows rockfall modelling from the slope height of 10 m with a slope angle of 65°.

A total of 243 simulations have been performed by varying the three sets of values for these five input parameters. Three-level values of the aforesaid five parameters were varied, usually referred to as low, intermediate and high values, as given in Table 2.

5 Parametric Analysis

A parametric analysis has been performed to observe the effects of rockfall input parameters on the rockfall output parameters. Further, multivariate linear regression has been used to develop the generalised

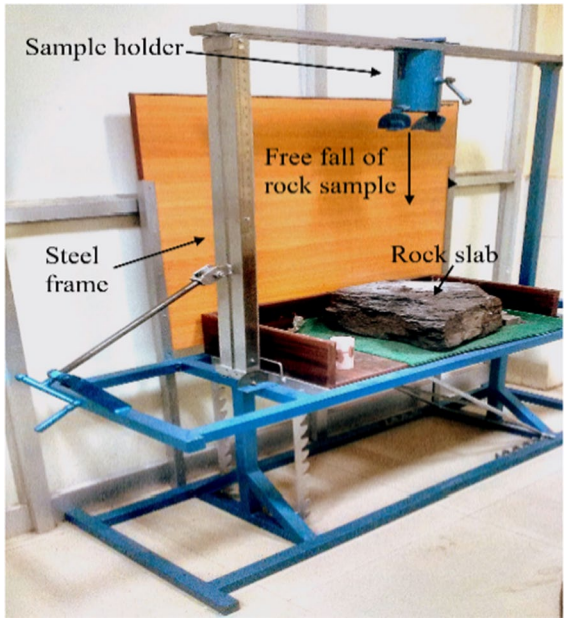

Fig. 6 Experimental setup to determine CoR values in the laboratory

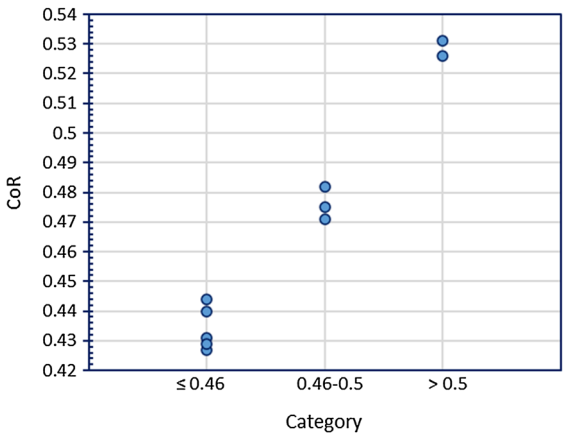

Fig. 7 CoR values estimated in the laboratory

equations to predict the rockfall outcome. One of the five input parameters was varied while keeping the other four constant to observe its influence on the output parameters. The procedure was repeated for each input parameter. A factorial design of experiments was used in the parametric study (Sinha 2013; Montgomery et al. 2011). In the factorial experiment with k factors (here, $k=5$), each factor has three levels of value (provided in Table 2), will need 3^k number of runs (i.e. $3^5 = 243$). This is recognized as 3^k factorial design and read as three-level 'k' factor design.

5.1 Factorial Plots for Bounce Height, Velocity and Kinetic

The factorial plots were plotted using the Minitab software package to observe the main effects among the rockfall input parameters for their different values on the rockfall output parameters. Figure 9 shows the main effect of slope height, slope angle, block weight, CoR and slope roughness on the bounce height, velocity and kinetic energy.

The factorial plots reveal that, for bounce height, the maximum variation is shown by slope-angle (Fig. 9a); therefore, slope-angle will influence the bounce height higher than the other four rockfall input parameters. Also, no variation was observed in block weight; hence, it will not affect the bounce height in any manner. The influence of slope roughness will be higher than the slope height and CoR, and lower than the slope angle. In the factorial velocity plots (Fig. 9b), slope height shows higher variation followed by slope angle, while the remaining three parameters were constant. Therefore, slope height is the major influencing input for the velocity of the rockfalls. For the factorial plot of kinetic energy (Fig. 9c), the major variation was observed by block weight and slope height. The slope angle also shows a minor variation. Therefore, these three inputs will affect the kinetic energy associated with the falling rock blocks.

5.2 Multivariate Linear Regression for Bounce Height, Velocity and Kinetic Energy

Multivariate linear regression analysis is used to develop the linear equations that can predict the bounce height, velocity and kinetic energy of

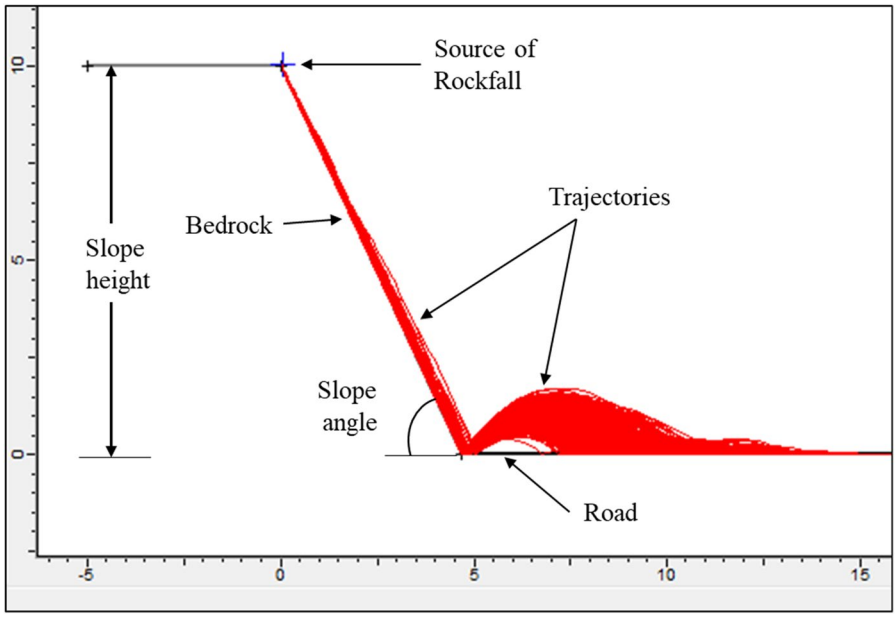

Fig. 8 Rockfall modelling showing the slope geometry, slope material, seeder point and trajectories of the falling rock blocks

rockfalls. The data used in the regression analysis has been generated through the 243 rockfall simulations. A linear form of regression was taken for analysis, as given in Eq. 2.

$$\text{Output} = a_1 + a_2 \times W + a_3 \times H_s + a_4 \times \theta + a_5 \times \text{CoR} + a_6 \times R_s \quad (2)$$

where, a_1 through a_7 are constants. The output parameters are *Bounce height, Kinetic energy* and *Velocity*. The linear regression analysis aims to find out the respective constants. Minitab software package was used to carry out regression analysis.

Table 2 Parameters with three levels of value (low, intermediate, and high) used in rockfall modelling and parametric study

S. No	Parameters	Lower value	Intermediate value	Higher value
1	Block weight (kg)	100	500	1000
2	Slope height (m)	10	20	30
3	Slope angle (deg)	65	75	85
4	CoR	0.43	0.48	0.53
5	Slope roughness	0	2	5

5.2.1 *Observation of the Results for Bounce Height, Velocity and Kinetic Energy*

The regression analysis was performed using 'Analysis of Variance' (ANOVA) (Table 3). The '*P*-value' in the last column of the ANOVA section of Tables 3, 4, 5 indicated the significance of the model. It represents the goodness of fit; the lower the value, the better the fit. The *P*-value must be lesser than 0.05 for the model to fit into the data. For all three outputs, bounce height, velocity and kinetic energy, its value is 0.00 (i.e. less than 0.05); therefore, the model is a good fit.

Similarly, for the coefficients section in Tables 3, 4, 5, *P*-value represents the significance of the variable coefficients. In case if *P*-value is higher than 0.05, it indicates that the coefficient estimate is not consistent as it would have too much variation or dispersion. The individual coefficients column gives the respective constants of the regression equation. Here, in *bounce height*, the '*P*-value' of all the parameters is

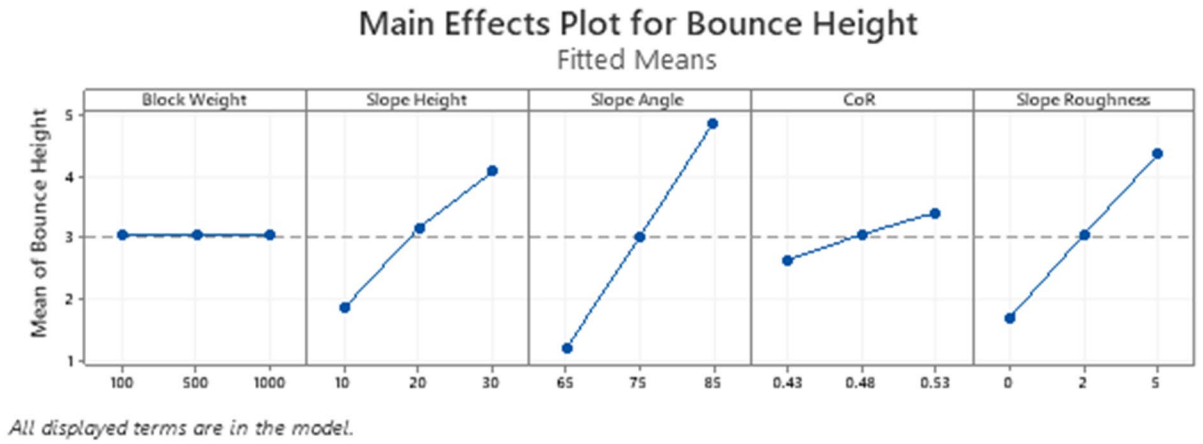

(a)

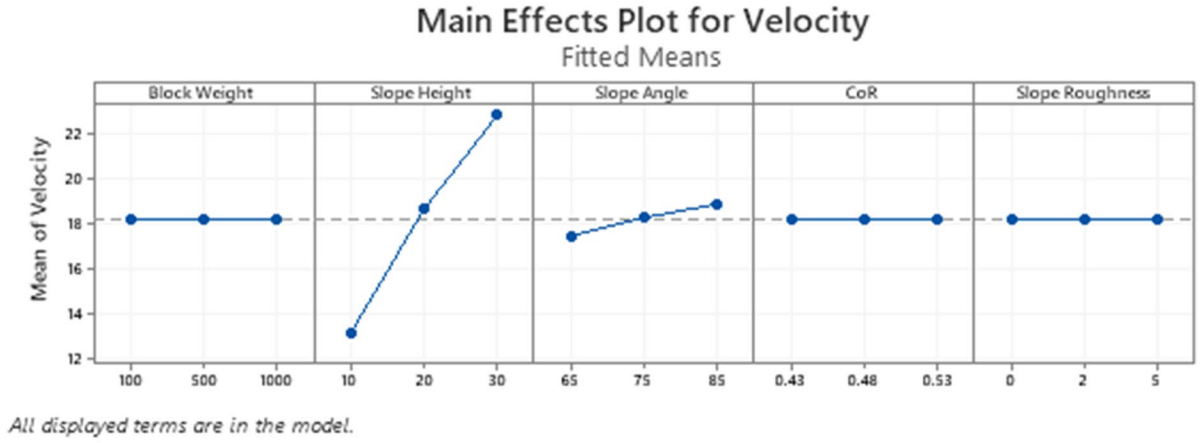

(b)

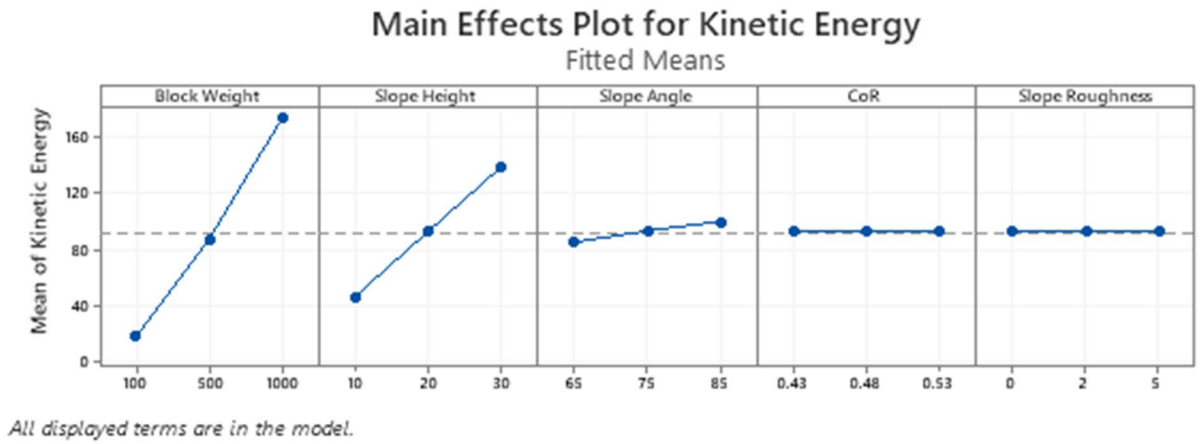

(c)

Fig. 9 Main effects plot for **a** bounce height, **b** velocity, and **c** kinetic energy associated with the falling rock blocks

Table 3 Result of regression analysis for bounce height versus parameters

Coefficients					
Term	Coef	SE Coef	T-value	*P*-value	VIF
Constant	− 17.87	1.18	− 15.16	0.000	
Block weight	0.00000	0.000210	0.00	1.000	1.00
Slope height	0.11056	0.00946	11.69	0.000	1.00
Slope angle	0.18304	0.00946	19.36	0.000	1.00
CoR	7.76	1.89	4.10	0.000	1.00
Slope roughness	0.5243	0.0376	13.95	0.000	1.00

Model summary			
S	R-sq %	R-sq (adj) %	R-sq (pred) %
1.20360	75.31	74.79	73.95

Analysis of variance					
Source	DF	Adj SS	Adj MS	F-value	*P*-value
Regression	5	1047.17	209.433	144.57	0.000
Block weight	1	0.00	0.000	0.00	1.000
Slope height	1	198.00	198.005	136.68	0.000
Slope angle	1	542.74	542.741	374.65	0.000
CoR	1	24.38	24.383	16.83	0.000
Slope roughness	1	282.33	282.036	194.69	0.000
Error	237	343.33	1.449		
Total	242	1390.50			

SS Sum of Squares; *MS* Mean Squared Errors; *VIF* Variance Inflation Factor; *SE* Standard Error; *DF* Degree of Freedom

0.000, except the 'block weight'. Therefore, the model is a good fit for the data, whereas the block weight parameter has wide variations and is not a good fit for the data. R-sq = 74.31% value indicates that one can predict *bounce height*'s value with 74.31% confidence. The value of R-sq (adj) = 74.79% suggests that this model can be used to explain 74.79% of the present data. In the *velocity*, the '*P*-value' for slope height and slope angle was less than 0.05, indicating the model is a good fit for the data. However, for the remaining three parameters, their values are higher than 0.05 (i.e.1.000, 0.980, and 0.992), indicating that these variables' coefficient estimates are less reliable than slope height and slope angle. In the *kinetic energy*, block weight, slope height and slope angle have *P*-values of 0.000 or 0.001, indicating that the model is a good fit. However, for the remaining two input parameters, its value was 0.992 and 1.000 (i.e. higher than 0.05). Hence, the coefficients for these two variables can be considered less reliable.

Figure 10 shows the residual plots of the regression analysis for rockfall output parameters. The two major plots are the normal probability plot and histogram plot. The purpose of a normal probability plot is to identify outliers of the data, whereas a histogram plot represents the distribution of the data. The outliers of data and distribution of the data for bounce height, velocity and kinetic energy have been shown in Fig. 10a–c respectively.

Table 4 Result of regression analysis for velocity versus parameters

Coefficients					
Term	Coef	SE coef	T-value	*P*-value	VIF
Constant	3.152	0.363	8.67	0.000	
Block weight	0.00000	0.000065	0.00	1.000	1.00
Slope height	0.48517	0.00292	166.36	0.000	1.00
Slope angle	0.07078	0.00292	24.27	0.000	1.00
CoR	− 0.015	0.583	− 0.03	0.980	1.00
Slope roughness	− 0.0001	0.0116	− 0.01	0.992	1.00

Model summary			
S	R-sq %	R-sq (adj) %	R-sq (pred) %
0.371183	99.17	99.15	99.13

Analysis of variance					
Source	DF	Adj SS	Adj MS	F-value	*P*-value
Regression	5	3894.42	778.88	5653.24	0.000
Block weight	1	0.00	0.00	0.00	1.000
Slope height	1	3813.26	3813.26	27,677.16	0.000
Slope angle	1	81.15	81.15	589.02	0.000
CoR	1	0.00	0.00	0.00	0.980
Slope roughness	1	0.00	0.00	0.00	0.992
Error	237	32.65	0.14		
Total	242	3927.07			

SS Sum of Squares; *MS* Mean Squared Errors; *VIF* Variance Inflation Factor; *SE* Standard Error; *DF* Degree of Freedom

5.2.2 Regression Equations

According to the regression analysis results in Tables 3 through 5, the coefficients of equations are substituted in Eq. 2 to derive the equations of bounce height, velocity and kinetic energy, respectively, for the rockfalls. These equations are given below (Eqs. 3 through 5).

$$\text{Bounce height} = -17.87 + 0.11 \times \text{H} + 0.18 \times \theta + 7.76 \times \text{CoR} + 0.52 \times \text{R}_\text{s} \left(\text{R}^2 = 75.31\right) \quad (3)$$

$$\text{Velocity} = 3.15 + 0.49 \times \text{H} + 0.07 \times \theta \left(\text{R}^2 = 99.17\right) \quad (4)$$

$$\text{Kinetic energy} = -147.4 + 0.17 \times \text{W} + 4.65 \times \text{H} + 0.73 \times \theta \left(\text{R}^2 = 88.53\right) \quad (5)$$

5.3 Statistical Validation of the Regression Equations

The validation has been performed by plotting the predicted values estimated from the developed equations versus values of output variables i.e. *bounce height, velocity* and *kinetic energy* observed through rockfall simulations and measuring its correlation. Plots of the correlation of the predicted versus observed values are given in Fig. 11a through 11c for *bounce height, velocity* and *energy,* respectively. The correlation coefficient $\left(\text{R}^2\right)$ of 0.78, 0.98 and 0.92 for *bounce height, velocity, and energy have been observed, respectively, indicating the confidence level with which these equations can*

Table 5 Result of regression analysis for kinetic energy versus parameters

Coefficients					
Term	Coef	SE Coef	T-value	*P*-value	VIF
Constant	− 147.4	26.5	− 5.55	0.000	
Block weight	0.17292	0.00472	36.62	0.000	1.00
Slope height	4.649	0.213	21.83	0.000	1.00
Slope angle	0.728	0.213	3.42	0.001	1.00
CoR	− 0.5	42.6	− 0.01	0.992	1.00
Slope roughness	− 0.000	0.846	− 0.00	1.000	1.00

Model summary			
S	R-sq %	R-sq (adj) %	R-sq (pred) %
27.1012	88.53	88.29	87.84

Analysis of variance					
Source	DF	Adj SS	Adj MS	F-value	*P*-value
Regression	5	1,343,583	268,717	356.86	0.000
Block weight	1	984,919	9,849,191	1340.98	0.000
Slope height	1	350,070	350,070	476.62	0.000
Slope angle	1	8594	8594	11.70	0.001
CoR	1	0	0	0.00	0.992
Slope roughness	1	0	0	0.00	1.000
Error	237	174,071	734		
Total	242	1,517,654			

SS Sum of Squares; *MS* Mean Squared Errors; *VIF* Variance Inflation Factor; *SE* Standard Error; *DF* Degree of Freedom

predict the output parameters for rockfall at specified locations.

6 Design Sample of Rockfall Barrier and Other Mitigative Measures

Vogel et al. (2009) explained selecting appropriate protective measures based on falling rock blocks' energy. The commonly used protective measures worldwide are benched slopes, ditches, rockfall barriers, gabion walls, nets, rock sheds, earth dams and reinforced dams (Fig. 12).

A rockfall barrier is one of the suitable preventive measures for rockfall hazards. The crucial properties to design a rockfall barrier are capacity (energy), height, inclination and location. The barrier's design can be achieved by equations proposed by (Peila and Ronco 2009).

According to the energy design equation, the energy absorbed by the barrier must be greater than the energy computed by the simulation program (Eq. 6).

$$E_d - \frac{E_{ETA}}{\gamma_E} < 0 \tag{6}$$

$$h_d > \left(h_{b95} \times \gamma_{Tr} \times \gamma_{Dp} + f_b\right) \tag{7}$$

where E_{ETA} is the energy of barrier certified by European Technical Approval (ETA), E_d is design energy for a barrier that can be computed through simulation, h_d is the design height of the barrier, h_{b95} is 95 percentile of the height of the trajectories of falling

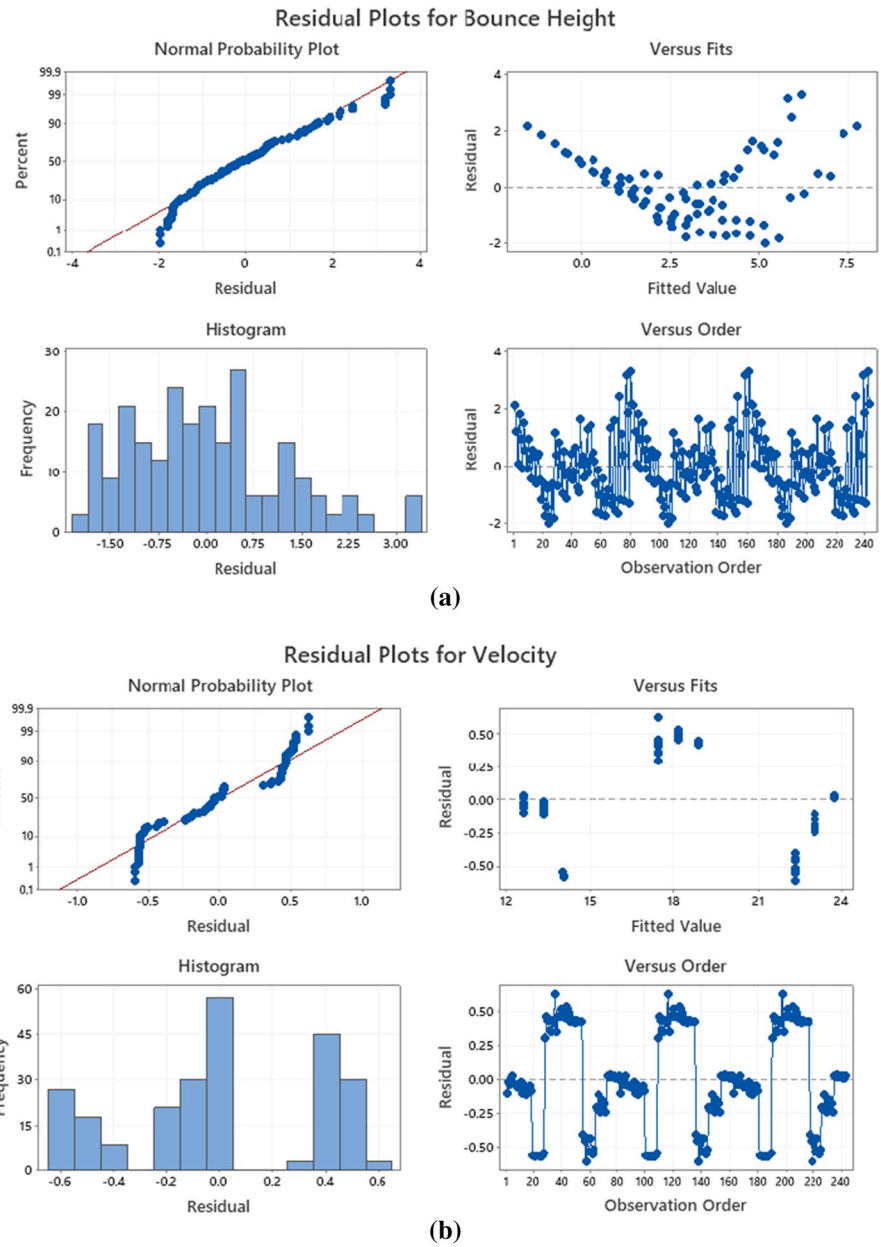

Fig. 10 Residual plot of the regression analysis for **a** bounce height, **b** velocity **c** kinetic energy associated with the falling rock blocks

rock blocks over the slope (i.e. bounce height), f_b is half of the average size of the falling rock block, γ_E, γ_{Tr} and γ_{Dp} are the safety factors concerning energy computation, trajectory computation and slope discretization quality, respectively.

The rockfall assessment conducted by Verma et al. (2018), using Rocfall software package, reveals that kinetic energy was estimated to be 58.2 kJ. Subsequently, using Eq. 6, the minimum barrier capacity was 75.7 kJ. Similarly, the bounce height was 1.4 m and using Eq. 7. The minimum barrier height was

Fig. 10 (continued)

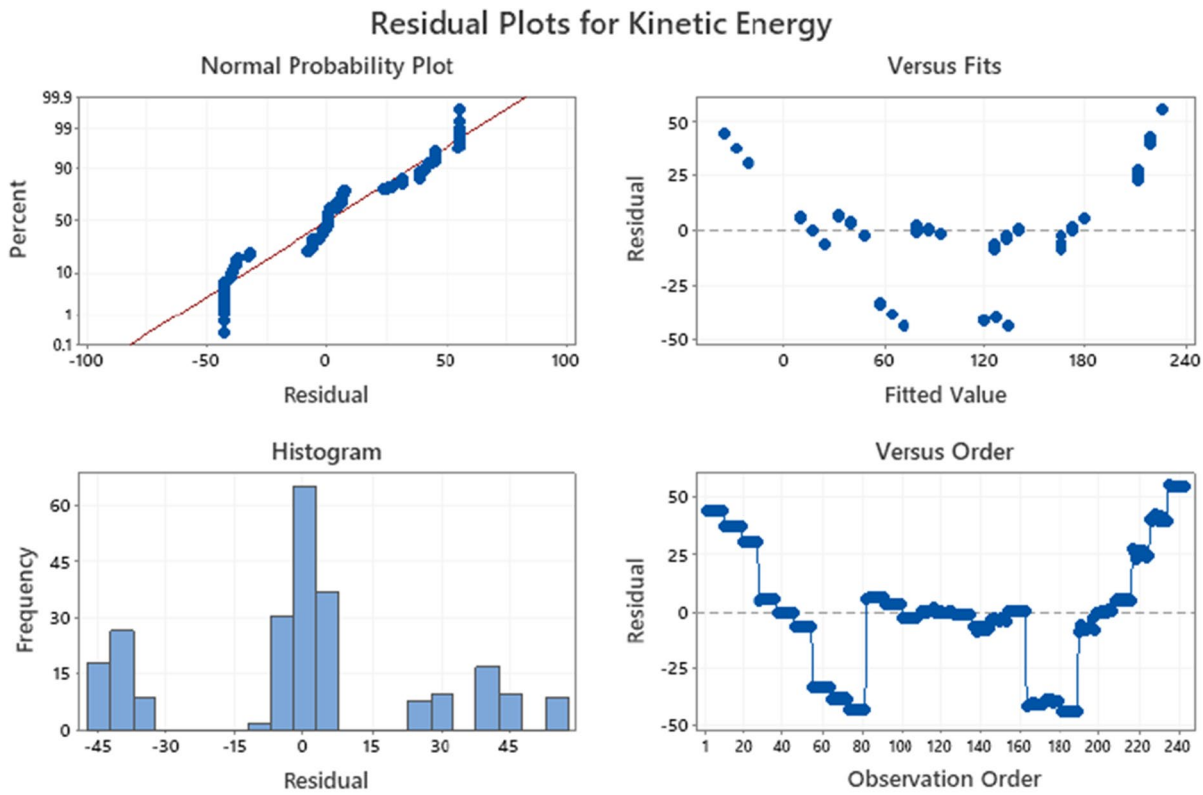

(c)

2.1 m. Therefore, a rockfall barrier of a minimum of 2.5 m in height and 100 kJ capacity was proposed to arrest all the falling blocks (Fig. 13a). Considering the same inputs parameters, the bounce height and kinetic energy calculated through Eqs. 3 and 5 were 1.5 m and 50.5 kJ, respectively. Further, using Eqs. 6 and 7, the minimum barrier height and capacity were 2.2 m and 65.6 kJ, respectively (Fig. 13b). The calculated values show a 5–13% variation between the present study and Verma et al. (2018). However, the overall proposed height and barrier capacity remain the same, i.e. 100 kJ of barrier capacity with a barrier height of 2.5 m.

The magnitude of energy and the bounce height can be estimated through Eqs. 3 and 5 instead of computing through the rockfall simulation package. Similarly, for selecting other energy-based protection structures suggested by Vogel et al. 2009, the energy magnitude can be estimated using Eq. 5.

7 Conclusion

The present study includes (i) the determination of input parameters through an extensive field investigation of 13 rock slopes carried out at the Lengpui-Aizawl highway, (ii) the testing carried out in the laboratory on collected rock samples from the site and (iii) a total of 243 simulations of rockfall by varying three level of values of five input parameters.

- The parametric analysis helps to identify the influence of each input parameter on the outcome of the rockfall. The results reveal that the slope-angle, slope-height and block-weight are three parameters that affect the bounce height,

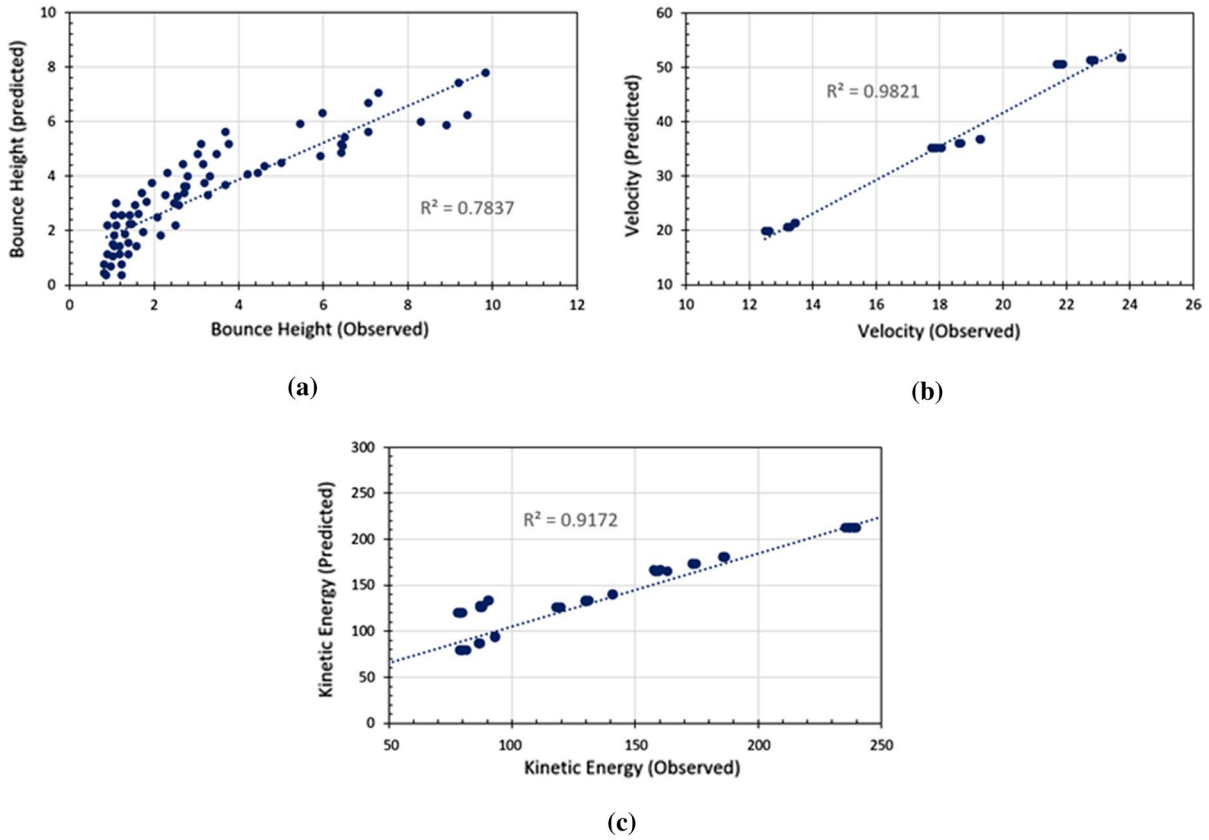

Fig. 11 Correlation of **a** bounce height **b** velocity **c** kinetic energy associated with the falling rock blocks

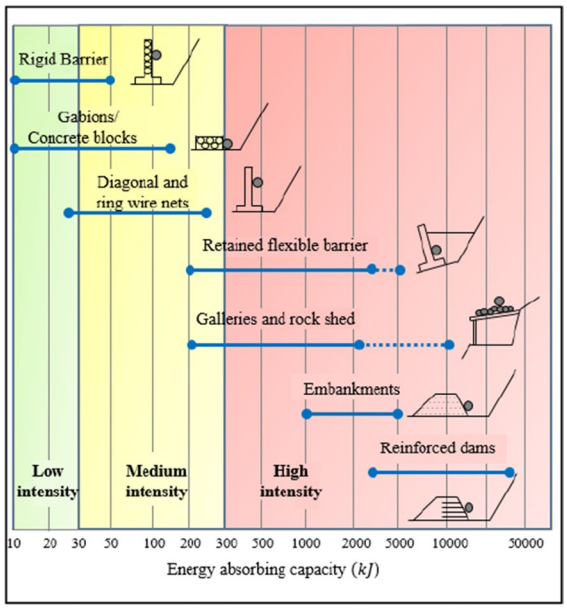

Fig. 12 Selection of various protection structures based on their energy absorbing capacity (after Vogel et al. 2009)

velocity and kinetic energy, respectively, compared to the rest of the input parameters.

- A set of generalised equations was developed and further validated using multivariate linear regression analysis to predict the bounce height, velocity, and kinetic energy associated with the rockfall activity.
- The assessment of rockfall using software packages is costly and time-consuming. Similar results (variation approximately up to 13%) were observed through the developed equations compared to the outcome of rockfall modelling. Further, these generalised equations will assist the field engineers in selecting and designing a suitable mitigative measure against rockfall.
- The study is limited to the rock slopes of NH-44A. The work can be further expanded by including more case studies from other parts of the country.

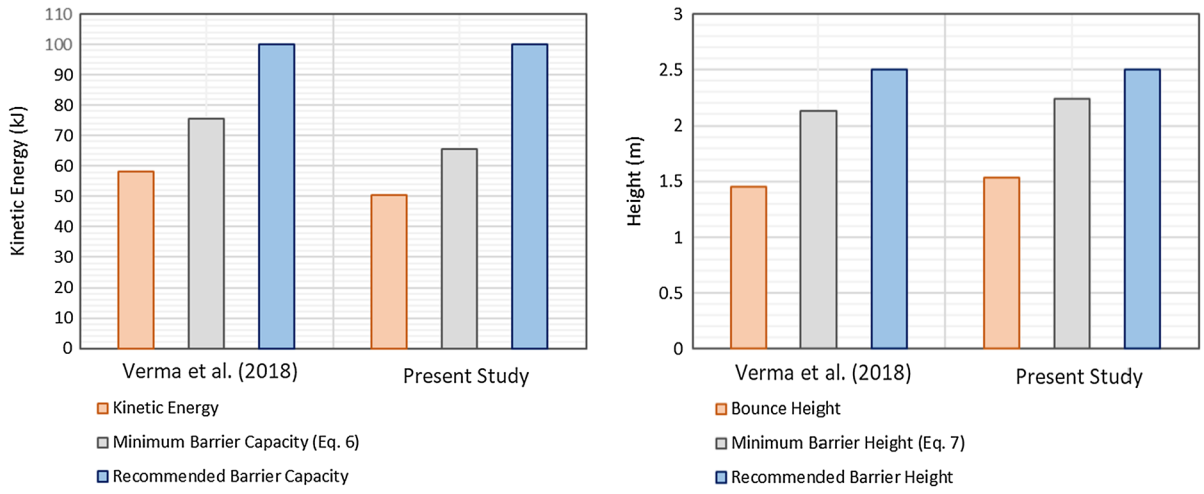

Fig. 13 Histogram plots showing a comparison of the present study with Verma et al. (2018) for **a** kinetic energy, and **b** bounce height

Acknowledgements The authors would like to thank the Ministry of Earth Science (MOES), Government of India, for the grant to carry out this study. The concerned personnel of various departments in IIT(ISM) Dhanbad are highly acknowledged.

Data Availability Enquiries about data availability should be directed to the authors.

Declarations

Conflicts of Interest The authors wish to confirm that there are no conflicts of interest with this research article.

References

Asteriou P (2019) Effect of impact angle and rotational motion of spherical blocks on the coefficients of restitution for rockfalls. Geotech Geol Eng 37(4):2523–2533

Asteriou P, Saroglou H, Tsiambaos G (2012) Geotechnical and kinematic parameters affecting the coefficients of restitution for rock fall analysis. Int J Rock Mech Min Sci 2012(54):103–113. https://doi.org/10.1016/j.ijrmms.2012.05.029

Badger T, Lowell S (1992) Rockfall control in Washington State. Transportation Research Record 1343, National Academy of Sciences, Washington, pp 14–19

Buzzi O, Giacomini A, Spadari M (2012) Laboratory investigation on high values of restitution coefficients. Rock Mech Rock Eng 45(1):35–43. https://doi.org/10.1007/s00603-011-0183-0

Dattola G, Crosta GB, di Prisco C (2021) Investigating the influence of block rotation and shape on the impact process. Int J Rock Mech Min Sci 147:104867

Ganju JL (1975) Geology of Mizoram. Bull Geol Min Met Soc India 48:17–26

Hoek E, Bray JW (1981) Rock slope engineering, 3rd edn. Institute of Mining and Metallurgy, London

Hoek E (1999) Putting numbers to geology - An engineer's viewpoint. Felsbau 17(3):139–151

Irfan M, Chen Y (2017) Segmented loop algorithm of theoretical calculation of trajectory of rockfall. Geotech Geol Eng 35(1):377–384

ISRM (1981) Suggested methods: rock characterization, testing and monitoring. ISRM Commission on Testing Methods Pergamon, Oxford

Jaswal M, Sinha RK, Sen P (2020) Delineation of phreatic surface in soil type slope—a comparative study using physical and numerical modeling. J Min Sci 56(3):494–504. https://doi.org/10.1134/S1062739120036787

Kesari GK (2011) Geology and mineral resources of Manipur, Mizoram, Nagaland and Tripura. Geological Survey of India, Government of India, Guwahati, pp 1–103.

Kumar N, Verma AK, Sardana S, Sarkar K, Singh TN (2018) Comparative analysis of limit equilibrium and numerical methods for prediction of a landslide. Bull Eng Geol Env 77(2):595–608. https://doi.org/10.1007/s10064-017-1183-4

Lallianthanga RK, Lalbiakmawia F, Lalramchuana F (2013) Landslide hazard zonation of Mamit Town, Mizoram, India using remote sensing and gis techniques. Int J Geol Earth Environ Sci 3(1):184–194

McCarroll D, Shakesby R, Matthews J (1998) Spatial and temporal patterns of late Holocene rockfall activity on a Norwegian talus slope: a lichenometric and simulation-modeling approach. Arctic Alpine Res 30:51–60

McColl S (2015) Landslide causes and triggers. In landslide hazards risks and disasters. Academic Press, pp 17–42
Montgomery DC, Runger GC, Hubele NF (2011) Engineering statistics, 5th edn. Wiley, USA
Peila D, Ronco C (2009) Technical Note: Design of rockfall net fences and the new ETAG 027 European guideline. Nat Hazards Earth Syst Sci 9(4):1291–1298. https://doi.org/10.5194/nhess-9-1291-2009
Peng B (2000) Rockfall trajectory analysis - parameter determination and application. Civil Engineering, June.
Ram J, Venkataraman B (1984) Tectonic framework and hydrocarbon prospects of Mizoram. Petrol Asia J 7(1):60–65
Richards L (1988) Rockfall protection: a review of current analytical and design methods. Secondo Ciclo Di Conferenze Di Meccanica Ed Ingegneria Delle Rocce, MIR, Politecnico Di Torino, 11:1–13
Ritchie AM (1963) Evaluation of rockfall and its control. In Highway Research Record 17, Stability of Rock Slopes, Highway Research Board, National Research Council, Washington, pp 13–28.
RocScience (2016) Statistical analysis of rockfalls: collision analysis verification manual. RocScience Inc., Toronto
Roth RA (1983) Factors affecting landslide-susceptibility in San Mateo county, California. Bull Assoc Eng Geol 20(4):353–372
Sardana S, Verma AK, Singh A, Laldinpuia. (2019a) Comparative analysis of rockmass characterization techniques for the stability prediction of road cut slopes along NH-44A, Mizoram, India. Bull Eng Geol Env 78(8):5977–5989. https://doi.org/10.1007/s10064-019-01493-3
Sardana S, Verma AK, Verma R, Singh TN (2019b) Rock slope stability along road cut of Kulikawn to Saikhamakawn of Aizawl, Mizoram India. Nat Hazards 99(2):753–767. https://doi.org/10.1007/s11069-019-03772-4
Sardana S, Sharma P, Verma AK, Singh TN (2020) A case study on the rockfall assessment and stability analysis along Lengpui-Aizawl highway, Mizoram India. Arab J Geosci. https://doi.org/10.1007/s12517-020-06196-8
Sinha R (2013) Influence of in situ stress on design of layout and support in bord and pillar workings. Thesis, Indian School of Mines, India
Srikanth M (2015) Analysis of rockfall trajectories and evaluation of concrete.
Valagussa A, Frattini P, Crosta GB (2014) Earthquake-induced rockfall hazard zoning. Eng Geol 182(PB):213–225
Verma AK, Sardana S, Singh TN, Kumar N (2018) Rockfall analysis and optimized design of rockfall barrier along a strategic road near Solang Valley, Himachal Pradesh India. Indian Geotech J 48(4):686–699. https://doi.org/10.1007/s40098-018-0330-6
Verma AK, Sardana S, Sharma P, Dinpuia L, Singh TN (2019) Investigation of rockfall-prone road cut slope near Lengpui Airport, Mizoram, India. J Rock Mech Geotech Eng 11(1):146–158. https://doi.org/10.1016/j.jrmge.2018.07.007
Verma AK, Sinha RK, Sardana S, Jaswal M, Singh TN (2021) Investigation into the rockfall hazard along Lengpui-Aizawl Highway, NH-44A, Mizoram, India. Indian Geotech J 1:98
Vogel T, Labiouse V, Masuya H (2009) Rockfall protection as an integral task. Struct Eng Int: J Int Assoc Bridge Struct Eng (IABSE) 19(3):304–312. https://doi.org/10.2749/101686609788957856
Wei LW, Chen H, Lee CF, Huang WK, Lin ML, Chi CC, Lin HH (2014) The mechanism of rockfall disaster: a case study from Badouzih, Keelung, in northern Taiwan. Eng Geol 183:116–126. https://doi.org/10.1016/j.enggeo.2014.10.008
Wu S (1985) Rockfall evaluation by computer simulation. Transportation Research Record, No.1031, pp 1–5
Wyllie D, Norrish N (1996) Stabilisation of rock slopes. In landslides: investigation and mitigation, transportation research board, national research council, special report, 247(474):500